

## A Low Cost Watt-Hour Energy Meter Based on the AD7755

By Anthony Collins

### INTRODUCTION

This application note describes a low-cost, high-accuracy watt-hour meter based on the AD7755. The meter described is intended for use in single phase, two-wire distribution systems. However the design can easily be adapted to suit specific regional requirements, e.g., in the United States power is usually distributed to residential customers as single-phase, three-wire.

The AD7755 is a low-cost, single-chip solution for electrical energy measurement. The AD7755 is comprised of two ADCs, reference circuit, and all the signal processing necessary for the calculation of real (active) power. The AD7755 also includes direct drive capability for electromechanical counters (i.e., the energy register), and has a high-frequency pulse output for calibration and communications purposes.

This application note should be used in conjunction with the AD7755 data sheet. The data sheet provides detailed information on the functionality of the AD7755 and will be referenced several times in this application note.

### DESIGN GOALS

The international Standard IEC1036 (1996-09) – *Alternating Current Watt-Hour Meters for Active Energy (Classes 1 and 2)*, was used as the primary specification for this design. For readers more familiar with the ANSI C12.16 specification, see the section at the end of this application note, which compares the IEC1036 and ANSI C12.16 standards. This section explains the key IEC1036 specifications in terms of their ANSI equivalents.

The design greatly exceeds this basic specification for many of the accuracy requirements, e.g., accuracy at unity-power factor and at low (PF = ±0.5) power factor. In addition, the dynamic range performance of the meter has been extended to 500. The IEC1036 standard specifies accuracy over a range of 5% Ib to I<sub>MAX</sub>—see Table I. Typical values for I<sub>MAX</sub> are 400% to 600% of Ib. Table I outlines the accuracy requirements for a static watt-hour meter. The current range (dynamic range) for accuracy is specified in terms of Ib (basic current).

Table I. Accuracy Requirements

Current Value <sup>1</sup>	PF <sup>2</sup>	Percentage Error Limits <sup>3</sup>	
		Class 1	Class 2
0.05 Ib ≤ I < 0.1 Ib	1	±1.5%	±2.5%
0.1 Ib ≤ I ≤ I <sub>MAX</sub>	1	±1.0%	±2.0%
0.1 Ib ≤ I ≤ 0.2 Ib	0.5 Lag	±1.5%	±2.5%
	0.8 Lead	±1.5%	
0.2 Ib ≤ I ≤ I <sub>MAX</sub>	0.5 Lag	±1.0%	±2.0%
	0.8 Lead	±1.0%	

#### NOTES

<sup>1</sup>The current ranges for specified accuracy shown in Table I are expressed in terms of the basic current (Ib). The basic current is defined in IEC1036 (1996-09) section 3.5.1.1 as the value of current in accordance with which the relevant performance of a direct connection meter is fixed. I<sub>MAX</sub> is the maximum current at which accuracy is maintained.

<sup>2</sup>Power Factor (PF) in Table I relates the phase relationship between the fundamental (45 Hz to 65 Hz) voltage and current waveforms. PF in this case can be simply defined as PF = cos(φ), where φ is the phase angle between pure sinusoidal current and voltage.

<sup>3</sup>Class index is defined in IEC1036 (1996-09) section 3.5.5 as the limits of the permissible percentage error. The percentage error is defined as:

$$\text{Percentage Error} = \frac{\text{Energy Registered by Meter} - \text{True Energy}}{\text{True Energy}} \times 100\%$$

The schematic in Figure 1 shows the implementation of a simple, low-cost watt-hour meter using the AD7755. A shunt is used to provide the current-to-voltage conversion needed by the AD7755 and a simple divider network attenuates the line voltage. The energy register (kWh) is a simple electromechanical counter that uses a two-phase stepper motor. The AD7755 provides direct drive capability for this type of counter. The AD7755 also provides a high-frequency output at the CF pin for the meter constant (3200 imp/kWh). Thus a high-frequency output is available at the LED and opto-isolator output. This high-frequency output is used to speed up the calibration process and provides a means of quickly verifying meter functionality and accuracy in a production environment. The meter is calibrated by varying the line voltage attenuation using the resistor network R5 to R14.

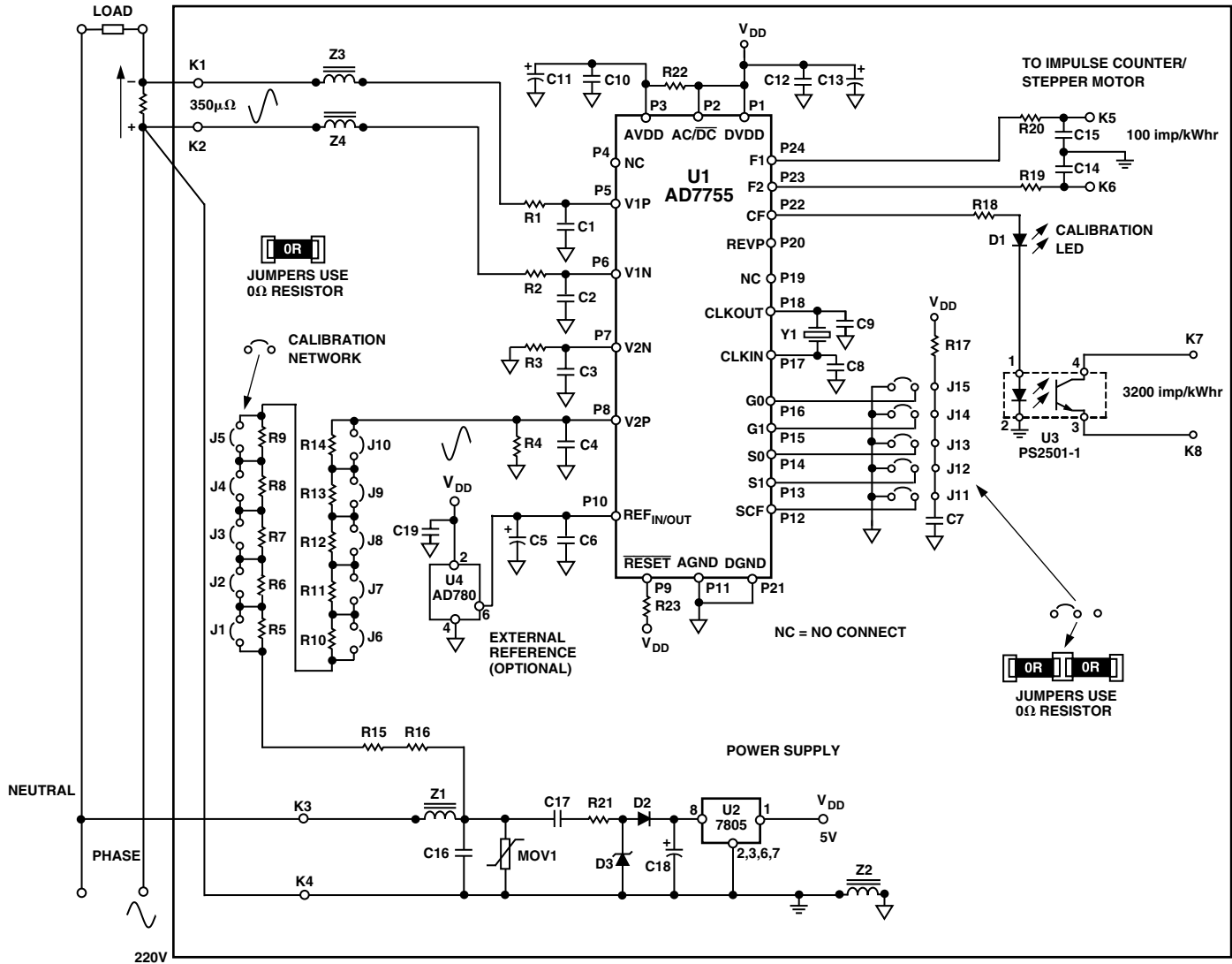


Figure 1. Simple Single-Phase Watt-Hour Meter Based on the AD7755

**DESIGN EQUATIONS**

The AD7755 produces an output frequency that is proportional to the time average value of the product of two voltage signals. The input voltage signals are applied at V1 and V2. The detailed functionality of the AD7755 is explained in the AD7755 data sheet, Theory Of Operation section. The AD7755 data sheet also provides an equation that relates the output frequency on F1 and F2 (counter drive) to the product of the rms signal levels at V1 and V2. This equation is shown here again for convenience and will be used to determine the correct signal scaling at V2 in order to calibrate the meter to a fixed constant.

$$Frequency = \frac{8.06 \times V1 \times V2 \times Gain \times F_{1-4}}{V_{REF}^2} \quad (1)$$

The meter shown in Figure 1 is designed to operate at a line voltage of 220 V and a maximum current ( $I_{MAX}$ ) of

40 A. However, by correctly scaling the signals on Channel 1 and Channel 2, a meter operating of any line voltage and maximum current could be designed.

The four frequency options available on the AD7755 will allow similar meters (i.e., direct counter drive) with an  $I_{MAX}$  of up to 120 A to be designed. The basic current ( $I_b$ ) for this meter is selected as 5 A and the current range for accuracy will be 2%  $I_b$  to  $I_{MAX}$ , or a dynamic range of 400 (100 mA to 40 A). The electromechanical register (kWh) will have a constant of 100 imp/kWh, i.e., 100 impulses from the AD7755 will be required in order to register 1 kWh. IEC1036 section 4.2.11 specifies that electromagnetic registers have their lowest values numbered in ten division, each division being subdivided into ten parts. Hence a display with a five plus one digits is used, i.e., 10,000s, 1,000s, 100s, 10s, 1s, 1/10s. The meter constant (for calibration and test) is selected as 3200 imp/kWh.

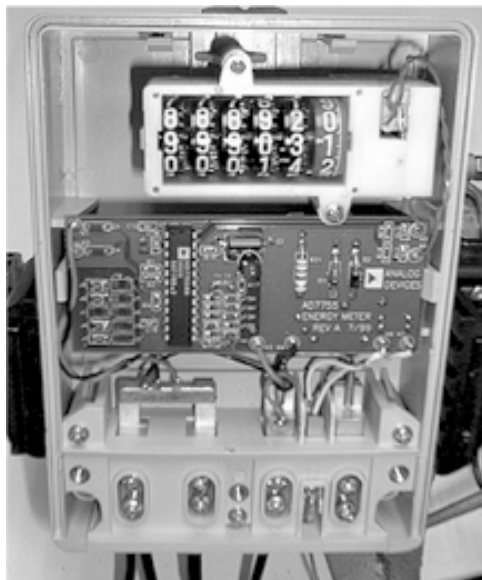


Figure 2. Final Implementation of the AD7755 Meter

#### AD7755 Reference

The schematic in Figure 1 also shows an optional reference circuit. The on-chip reference circuit of the AD7755 has a temperature coefficient of typically 30 ppm/°C. However, on A Grade parts this specification is not guaranteed and may be as high as 80 ppm/°C. At 80 ppm/°C the AD7755 error at -20°C/+60°C could be as high as 0.65%, assuming a calibration at 25°C.

#### Shunt Selection

The shunt size (350  $\mu\Omega$ ) is selected to maximize the use of the dynamic range on Channel V1 (current channel). However there are some important considerations when selecting a shunt for an energy metering application. First, minimize the power dissipation in the shunt. The maximum rated current for this design is 40 A, therefore, the maximum power dissipated in the shunt is  $(40 \text{ A})^2 \times 350 \mu\Omega = 560 \text{ mW}$ . IEC1036 calls for a maximum power dissipation of 2 W (including power supply). Secondly, the higher power dissipation may make it difficult to manage the thermal issues. Although the shunt is manufactured from Manganin material, which is an alloy with a low temperature coefficient of resistance, high temperatures may cause significant error at heavy loads. A third consideration is the ability of the meter to resist attempts to tamper by shorting the phase circuit. With a very low value of shunt resistance the effects of externally shorting the shunt are very much minimized. Therefore, the shunt should always be made as small as possible, but this must be offset against the signal range on V1 (0 mV–20 mV rms with a gain of 16). If the shunt is made too small it will not be possible to meet the IEC1036 accuracy requirements at light loads. A shunt value of 350  $\mu\Omega$  was considered a good compromise for this design.

#### Design Calculations

Design parameters:

Line voltage = 220 V (nominal)

$I_{MAX} = 40 \text{ A}$  ( $I_b = 5 \text{ A}$ )

Counter = 100 imp/kWh

Meter constant = 3200 imp/kWh

Shunt size = 350  $\mu\Omega$

100 imp/hour = 100/3600 sec = 0.027777 Hz

Meter will be calibrated at  $I_b$  (5A)

Power dissipation at  $I_b = 220 \text{ V} \times 5 \text{ A} = 1.1 \text{ kW}$

Frequency on F1 (and F2) at  $I_b = 1.1 \times 0.027777 \text{ Hz}$   
= 0.0305555 Hz

Voltage across shunt (V1) at  $I_b = 5 \text{ A} \times 350 \mu\Omega = 1.75 \text{ mV}$ .

To select the  $F_{1-4}$  frequency for Equation 1 see the AD7755 data sheet, Selecting a Frequency for an Energy Meter Application section. From Tables V and VI in the AD7755 data sheet it can be seen that the best choice of frequency for a meter with  $I_{MAX} = 40 \text{ A}$  is 3.4 Hz ( $F_2$ ). This frequency selection is made by the logic inputs S0 and S1—see Table II in the AD7755 data sheet. The CF frequency selection (meter constant) is selected by using the logic input SCF. The two available options are  $64 \times F_1$  (6400 imp/kWh) or  $32 \times F_1$  (3200 imp/kWh). For this design, 3200 imp/kWh is selected by setting SCF logic low. With a meter constant of 3200 imp/kWh and a maximum current of 40 A, the maximum frequency from CF is 7.82 Hz. Many calibration benches used to verify meter accuracy still use optical techniques. This limits the maximum frequency that can be reliably read to about 10 Hz. The only remaining unknown from equation 1 is V2 or the signal level on Channel 2 (the voltage channel).

From Equation 1 on the previous page:

$$0.030555 \text{ Hz} = \frac{8.06 \times 1.75 \text{ mV} \times V2 \times 16 \times 3.4 \text{ Hz}}{2.5^2}$$

$$V2 = 248.9 \text{ mV rms}$$

Therefore, in order to calibrate the meter the line voltage needs to be attenuated down to 248.9 mV.

#### CALIBRATING THE METER

From the previous section it can be seen that the meter is simply calibrated by attenuating the line voltage down to 248.9 mV. The line voltage attenuation is carried out by a simple resistor divider as shown in Figure 3. The attenuation network should allow a calibration range of at least  $\pm 30\%$  to allow for shunt tolerances and the on-chip reference tolerance of  $\pm 8\%$ —see AD7755 data sheet. In addition, the topology of the network is such that the phase-matching between Channel 1 and Channel 2 is preserved, even when the attenuation is being adjusted (see Correct Phase Matching Between Channels section).

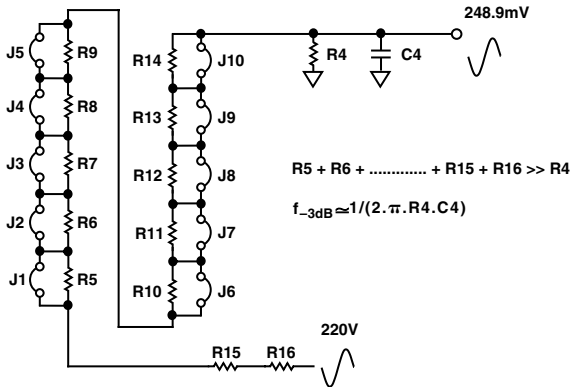


Figure 3. Attenuation Network

As can be seen from Figure 3, the -3 dB frequency of this network is determined by R4 and C4. Even with all the jumpers closed, the resistance of R15 (330 kΩ) and R16 (330 kΩ) is still much greater than R4 (1 kΩ). Hence varying the resistance of the resistor chain R5 to R14 will have little effect on the -3 dB frequency of the network. The network shown in Figure 3 allows the line voltage to be attenuated and adjusted in the range 175 mV to 333 mV with a resolution of 10 bits or 154 μV. This is achieved by using the binary weighted resistor chain R5 to R14. This will allow the meter to be accurately calibrated using a successive approximation technique. Starting with J1, each jumper is closed in order of ascendance, e.g., J1, J2, J3, etc. If the calibration frequency on CF, i.e., 32 × 100 imp/hr (0.9777 Hz), is exceeded when any jumper is closed, it should be opened again. All jumpers are tested, J10 being the last jumper. Note jumper connections are made with 0 Ω fixed resistors which are soldered into place. This approach is preferred over the use of trim pots, as the stability of the latter over time and environmental conditions is questionable.

Since the AD7755 transfer function is extremely linear a one-point calibration (1b) at unity power factor, is all that is needed to calibrate the meter. If the correct precautions have been taken at the design stage, no calibration will be necessary at low-power factor (PF = 0.5). The next section discusses phase matching for correct calculation of energy at low-power factor.

**CORRECT PHASE MATCHING BETWEEN CHANNELS**

The AD7755 is internally phase-matched over the frequency range 40 Hz to 1 kHz. Correct phase matching is important in an energy metering application because any phase mismatch between channels will translate into significant measurement error at low-power factor. This is easily illustrated with the following example. Figure 4 shows the voltage and current waveforms for an inductive load. In the example shown, the current lags the voltage by 60° (PF = -0.5). Assuming pure sinusoidal conditions, the power is easily calculated as  $V_{rms} \times I_{rms} \times \cos(60^\circ)$ .

If, however, a phase error ( $\phi_e$ ) is introduced externally to the AD7755, e.g., in the antialias filters, the error is calculated as:

$$[\cos(\delta^\circ) - \cos(\delta^\circ + \phi_e)] / \cos(\delta^\circ) \times 100\% \tag{2}$$

See Note 3 on Table I. Where  $\delta$  is the phase angle between voltage and current and  $\phi_e$  is the external phase error. With a phase error of 0.2°, for example, the error at PF = 0.5 (60°) is calculated as 0.6%. As this example demonstrates, even a very small phase error will produce a large measurement error at low power factor.

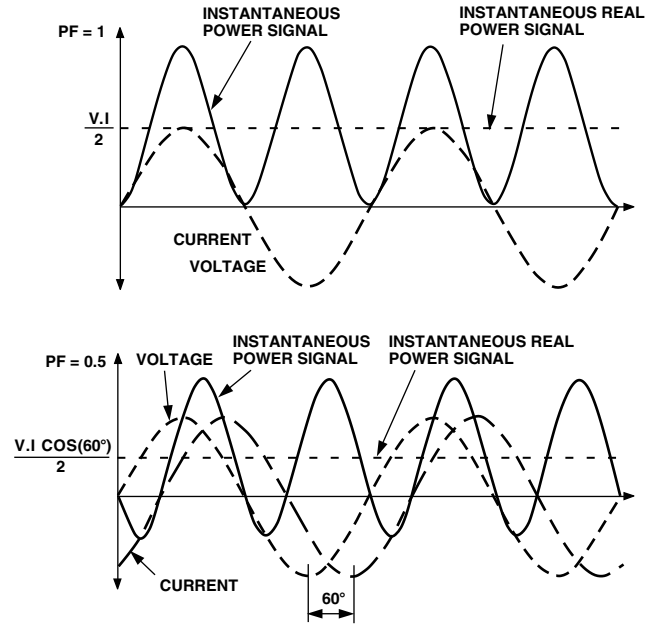


Figure 4. Voltage and Current (Inductive Load)

**ANTI\_ALIAS FILTERS**

As mentioned in the previous section, one possible source of external phase errors are the antialias filters on Channel 1 and Channel 2. The antialias filters are low-pass filters that are placed before the analog inputs of any ADC. They are required to prevent a possible distortion due to sampling called aliasing. Figure 5 illustrates the effects of aliasing.

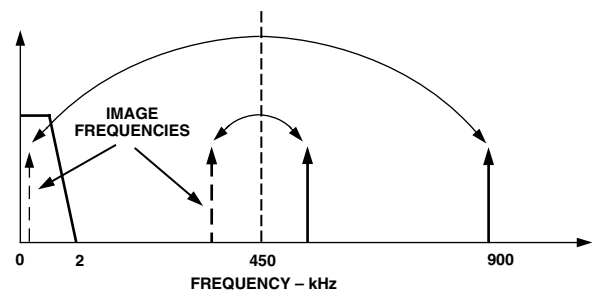


Figure 5. Aliasing Effects

Figure 5 shows how aliasing effects could introduce inaccuracies in an AD7755-based meter design. The AD7755 uses two  $\Sigma$ - $\Delta$  ADCs to digitize the voltage and current signals. These ADCs have a very high sampling rate, i.e., 900 kHz. Figure 5 shows how frequency components (arrows shown in black) above half the sampling frequency (also known as the Nyquist frequency), i.e., 450 kHz is imaged or folded back down below 450 kHz (arrows shown dashed). This will happen with all ADCs no matter what the architecture. In the example shown it can be seen that only frequencies near the sampling frequency, i.e., 900 kHz, will move into the band of interest for metering, i.e., 0 kHz–2 kHz. This fact will allow us to use a very simple LPF (Low-Pass Filter) to attenuate these high frequencies (near 900 kHz) and so prevent distortion in the band of interest.

The simplest form of LPF is the simple RC filter. This is a single-pole filter with a roll-off or attenuation of  $-20$  dB/dec.

#### Choosing the Filter $-3$ dB Frequency

As well as having a magnitude response, all filters also have a phase response. The magnitude and phase response of a simple RC filter ( $R = 1$  k $\Omega$ ,  $C = 33$  nF) are shown in Figures 6 and 7. From Figure 6 it is seen that the attenuation at 900 kHz for this simple LPF is greater than 40 dBs. This is enough attenuation to ensure no ill effects due to aliasing.

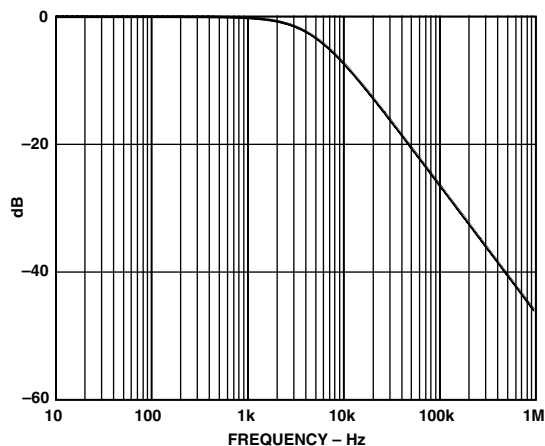


Figure 6. RC Filter Magnitude Response

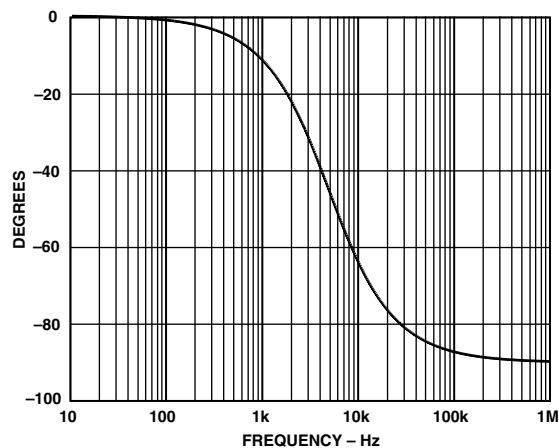


Figure 7. RC Filter Phase Response

As explained in the last section, the phase response can introduce significant errors if the phase response of the LPFs on both Channel 1 and Channel 2 are not matched. Phase mismatch can easily occur due to poor component tolerances in the LPF. The lower the  $-3$  dB frequency in the LPF (antialias filter) the more pronounced these errors will be at the fundamental frequency component or the line frequency. Even with the corner frequency set at 4.8 kHz ( $R = 1$  k $\Omega$ ,  $C = 33$  nF) the phase errors due to poor component tolerances can be significant. Figure 8 illustrates the point. In Figure 8, the phase response for the simple LPF is shown at 50 Hz for  $R = 1$  k $\Omega \pm 10\%$ ,  $C = 33$  nF  $\pm 10\%$ . Remember a phase shift of  $0.2^\circ$  can cause measurement errors of 0.6% at low-power factor. This design uses resistors of 1% tolerance and capacitors of 10% tolerance for the antialias filters to reduce the possible problems due to phase mismatch. Alternatively the corner frequency of the antialias filter could be pushed out to 10 kHz–15 Hz. However, the corner frequency should not be made too high, as this could allow enough high-frequency components to be aliased and so cause accuracy problems in a noisy environment.

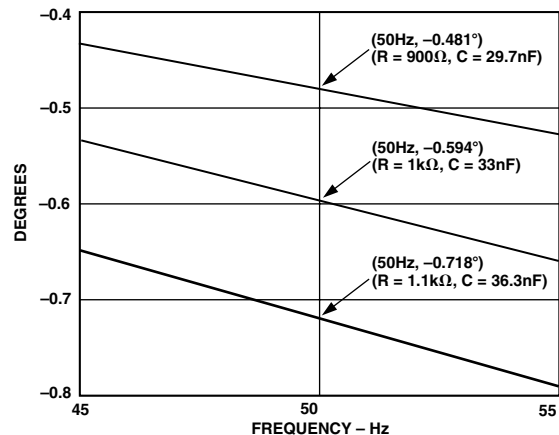


Figure 8. Phase Shift at 50 Hz Due to Component Tolerances

Note that this is also why precautions were taken with the design of the calibration network on Channel 2 (voltage channel). Calibrating the meter by varying the resistance of the attenuation network will not vary the -3 dB frequency and hence the phase response of the network on Channel 2—see Calibrating the Meter section. Shown in Figure 9 is a plot of phase lag at 50 Hz when the resistance of the calibration network is varied from 660 kΩ (J1-J10 closed) to 1.26 MΩ (J1-J10 open).

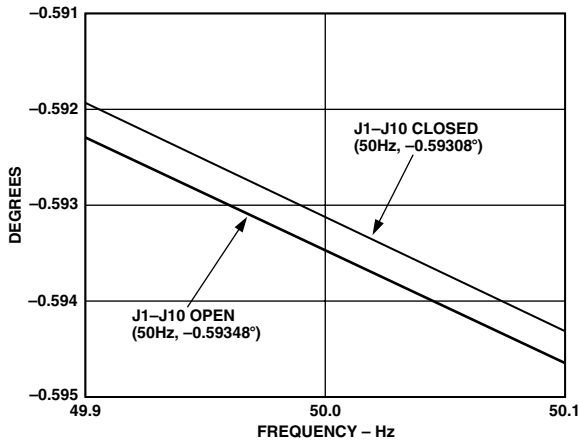


Figure 9. Phase Shift Due to Calibration

**COMPENSATING FOR PARASITIC SHUNT INDUCTANCE**

When used at low frequencies a shunt can be considered a purely resistive element with no significant reactive elements. However, under certain situations even a small amount of stray inductance can cause undesirable effects when a shunt is used in a practical data acquisition system. The problem is very noticeable when the resistance of the shunt is very low, in the order of 200 μΩ. Shown below is an equivalent circuit for the shunt used in the AD7755 reference design. There are three connections to the shunt. One pair of connections provides the current sense inputs (V1P and V1N) and the third connection is the ground reference for the system.

The shunt resistance is shown as  $R_{SH1}$  (350 μΩ).  $R_{SH2}$  is the resistance between the V1N input terminal and the system ground reference point. The main parasitic elements (inductance) are shown as  $L_{SH1}$  and  $L_{SH2}$ . Figure 10 also shows how the shunt is connected to the AD7755 inputs (V1P and V1N) through the antialias filters. The function of the antialias filters is explained in the previous section and their ideal magnitude and phase responses are shown in Figures 6 and 7.

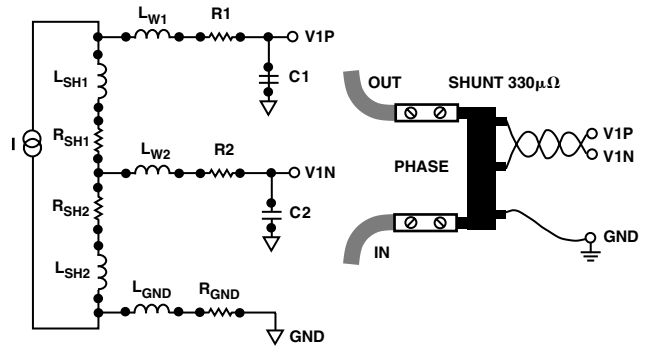


Figure 10. Equivalent Circuit for the Shunt

**Canceling the Effects of the Parasitic Shunt Inductance**

The effect of the parasitic shunt inductance is shown in Figure 11. The plot shows the phase and magnitude response of the antialias filter network with and without (dashed) a parasitic inductance of 2 nH. As can be seen from the plot, both the gain and phase response of the network are affected. The attenuation at 1 MHz is now only about -15 dB, which could cause some repeatability and accuracy problems in a noisy environment. More importantly, a phase mismatch may now exist between the current and voltage channels. Assuming the network on Channel 2 has been designed to match the ideal phase response of Channel 1, there now exists a phase mismatch of 0.1° at 50 Hz. Note that 0.1° will cause a 0.3% measurement error at PF = ±0.5. See Equation 2 (Correct Phase Matching Between Channels).

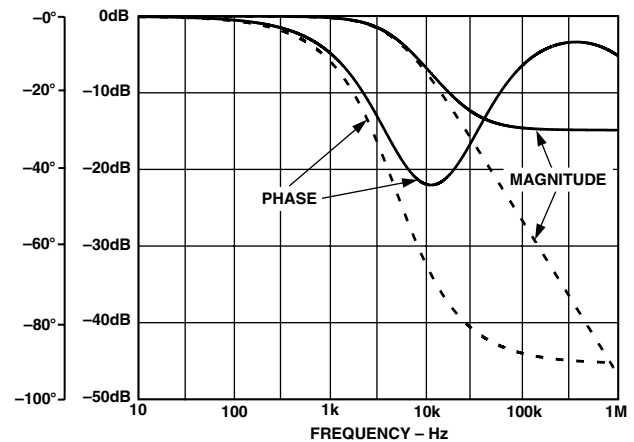


Figure 11. Effect of Parasitic Shunt Inductance on the Antialias Network

The problem is caused by the addition of a zero into the antialias network. Using the simple model for the shunt shown in Figure 10, the location of the zero is given as  $R_{SH1}/L_{SH1}$  radians.

One way to cancel the effects of this additional zero in the network is to add an additional pole at (or close to) the same location. The addition of an extra RC on each analog input of Channel 1 will achieve the additional

pole required. The new antialias network for Channel 1 is shown in Figure 12. To simplify the calculation and demonstrate the principle, the Rs and Cs of the network are assumed to have the same value.

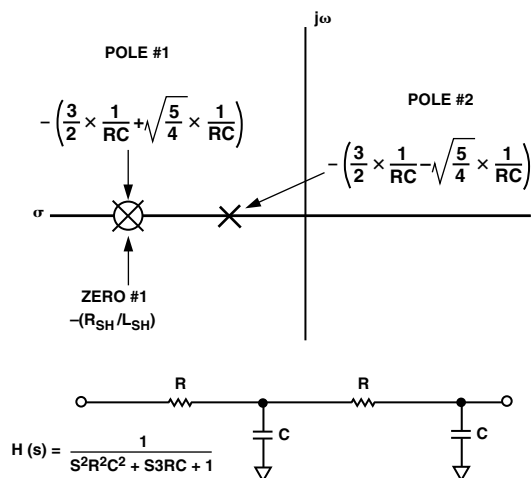


Figure 12. Shunt Inductance Compensation Network

Figure 12 also gives an expression for the location of the poles of this compensation network. The purpose of Pole #1 is to cancel the effects of the zero due to the shunt inductance. Pole #2 will perform the function of the antialias filters as described in the Antialias Filters section. The following illustrates a sample calculation for a shunt of 330  $\mu\Omega$  with a parasitic inductance of 2 nH.

The location of the pole #1 is given as:

$$-\left(\frac{3}{2} \times \frac{1}{RC} + \sqrt{\frac{5}{4}} \times \frac{1}{RC}\right) = \frac{R_{SH1}}{L_{SH1}}$$

For  $R_{SH1} = 330 \mu\Omega$ ,  $L_{SH1} = 2 \text{ nH}$ ,  $C = 33 \text{ nF}$

$R$  is calculated as approximately 480  $\Omega$  (use 470  $\Omega$ ).

The location of Pole #1 is 165,000 rads or 26.26 kHz.

This places the location of Pole # 2 at:

$$-\left(\frac{3}{2} \times \frac{1}{RC} + \sqrt{\frac{5}{4}} \times \frac{1}{RC}\right) = 3.838 \text{ kHz}$$

To ensure phase-matching between Channel 1 and Channel 2, the pole at Channel 2 must also be positioned at this location. With  $C = 33 \text{ nF}$ , the new value of resistance for the antialias filters on Channel 2 is approximately 1.23 k $\Omega$  (use 1.2 k $\Omega$ ).

Figure 13 shows the effect of the compensation network on the phase and magnitude response of the antialias network in Channel 1. The dashed line shows the response of Channel 2 using practical values for the

newly calculated component values, i.e., 1.2 k $\Omega$  and 33 nF. The solid line shows the response of Channel 1 with the parasitic shunt inductance included. Notice phase and magnitude responses match very closely with the ideal response—shown as a dashed line. This is the objective of the compensation network.

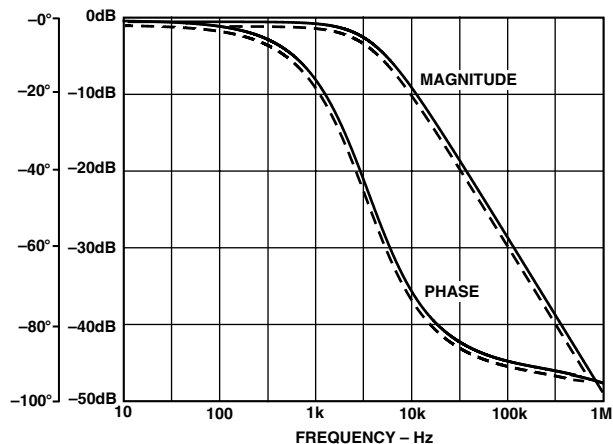


Figure 13. Antialias Network Phase and Magnitude Response after Compensation

The method of compensation works well when the pole due to shunt inductance is less than 25 kHz or so. If zero is at a much higher frequency its effects may simply be eliminated by placing an extra RC on Channel 1 with a pole that is a decade greater than that of the antialias filter, e.g., 100  $\Omega$  and 33 nF.

Care should be taken when selecting a shunt to ensure its parasitic inductance is small. This is especially true of shunts with small values of resistance, e.g., <200  $\mu\Omega$ . Note that the smaller the shunt resistance, the lower the zero frequency for a given parasitic inductance (Zero =  $R_{SH1}/L_{SH1}$ ).

## POWER SUPPLY DESIGN

This design uses a simple low-cost power supply based on a capacitor divider network, i.e., C17 and C18. Most of the line voltage is dropped across C17, a 470 nF 250 V metalized polyester film capacitor. The impedance of C17 dictates the effective VA rating of the supply. However the size of C17 is constrained by the power consumption specification in IEC1036. The total power consumption in the voltage circuit, including power supply, is specified in section 4.4.1.1 of IEC1036 (1996-9). The total power consumption in each phase is 2 W and 10 VA under nominal conditions. The nominal VA rating of the supply in this design is 7 VA. The total power dissipation is approximately 0.5 W. Together with the power dissipated in the shunt at 40 A load, the total power consumption of the meter is 1.06 W. Figure 14 shows the basic power supply design.

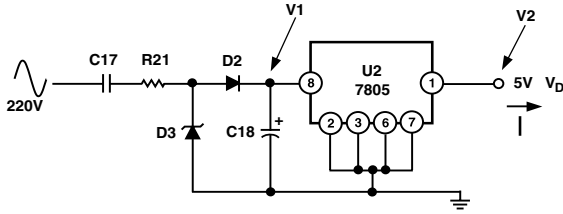


Figure 14. Power Supply

The plots shown in Figures 15, 16, 17, and 18 show the PSU performance under heavy load (50 A) with the line voltage varied from 180 V to 250 V. By far the biggest load on the power supply is the current required to drive the stepper motor which has a coil impedance of about 400 Ω. This is clearly seen by looking at V1 (voltage on C18) in the plots below. Figure 16 shows the current drawn from the supply. Refer to Figure 14 when reviewing the simulation plots below.

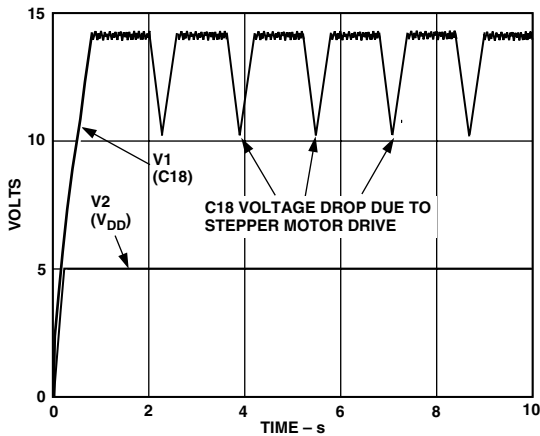


Figure 15. Power Supply Voltage Output at 220 V and 50 A Load

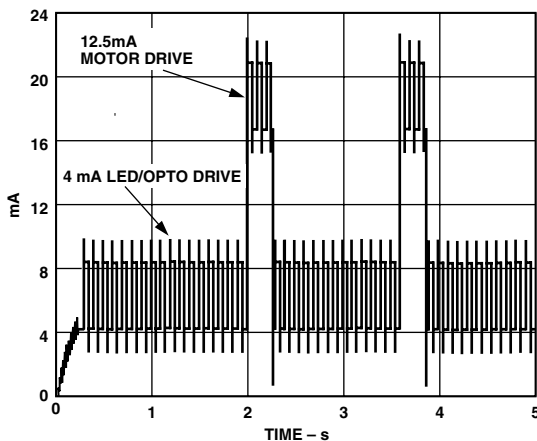


Figure 16. Power Supply Current Output at 220 V and 50 A Load

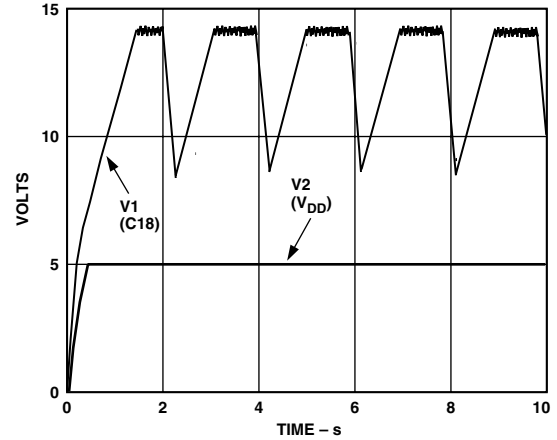


Figure 17. Power Supply Voltage Output at 180 V and 50 A Load

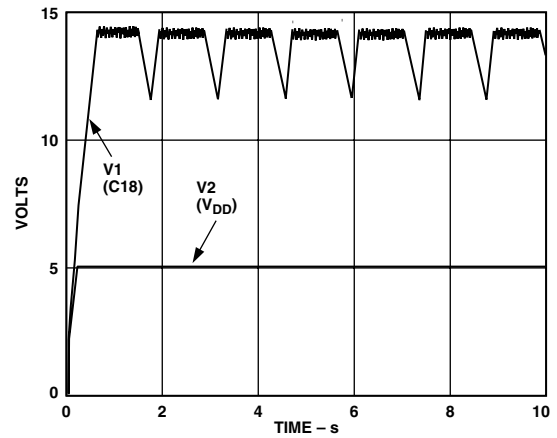


Figure 18. Power Supply Voltage Output at 250 V and 50 A Load

**DESIGN FOR IMMUNITY TO ELECTROMAGNETIC DISTURBANCE**

In Section 4.5 of IEC1036 it is stated that “the meter shall be designed in such a way that conducted or radiated electromagnetic disturbances as well as electrostatic discharge do not damage nor substantially influence the meter.” The considered disturbances are:

1. Electrostatic Discharge
2. Electromagnetic HF Fields
3. Fast Transience Burst

All of the precautions and design techniques (e.g., ferrite beads, capacitor line filters, physically large SMD resistors, PCB layout including grounding) contribute to a certain extent in protecting the meter electronics from each form of electromagnetic disturbance. Some precautions (e.g., ferrite beads), however, play a more important role in the presence of certain kinds of disturbances (e.g., RF and fast transience burst). The following discusses each of the disturbances listed above and details what protection has been put in place.



## ELECTROSTATIC DISCHARGE (ESD)

Although many sensitive electronic components contain a certain amount of ESD protection on-chip, it is not possible to protect against the kind of severe discharge described below. Another problem is that the effect of an ESD discharge is cumulative, i.e., a device may survive an ESD discharge, but it is no guarantee that it will survive multiple discharges at some stage in the future. The best approach is to eliminate or attenuate the effects of the ESD event before it comes in contact with sensitive electronic devices. This holds true for all conducted electromagnetic disturbances. This test is carried out according to IEC1000-4-2, under the following conditions:

- Contact Discharge;
- Test Severity Level 4;
- Test Voltage 8 kV;
- 10 Discharges.

Very often no additional components are necessary to protect devices. With a little care those components already required in the circuit can perform a dual role. For example, the meter must be protected from ESD events at those points where it comes in contact with the “outside world,” e.g., the connection to the shunt. Here the AD7755 is connected to the shunt via two LPFs (antialias filters) which are required by the ADC—see Antialias Filters section. This RC filter can also be enough to protect against ESD damage to CMOS devices. However, some care must be taken with the type of components used. For example, the resistors should not be wire-wound as the discharge will simply travel across them. The resistors should also be physically large to stop the discharge arcing across the resistor. In this design 1/8W SMD 1206 resistors were used in the antialias filters. Two ferrite beads are also placed in series with the connection to the shunt. A ferrite choke is particularly effective at slowing the fast rise time of an ESD current pulse. The high-frequency transient energy is absorbed in the ferrite material rather than being diverted or reflected to another part of the system. (*The properties of ferrite are discussed later.*) The PSU circuit is also directly connected to the terminals of the meter. Here the discharge will be dissipated by the ferrite, the line filter capacitor (C16), and the rectification diodes D2 and D3. The analog input V2P is protected by the large impedance of the attenuation network used for calibration.

Another very common low-cost technique employed to arrest ESD events is to use a spark gap on the component side of the PCB—see Figure 19. However, since the meter will likely operate in an open air environment and be subject to many discharges, this is not recommended at sensitive nodes like the shunt connection. Multiple

discharges could cause carbon buildup across the spark gap which could cause a short or introduce an impedance that will in time affect accuracy. A spark gap was introduced in the PSU after the MOV to take care of any very high amplitude/fast rise time discharges.

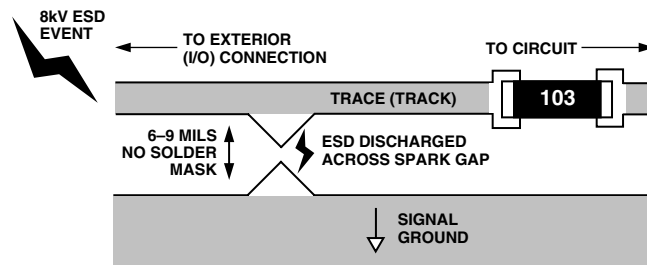


Figure 19. Spark Gap to Arrest ESD Events

## ELECTROMAGNETIC HF FIELDS

Testing is carried out according to IEC100-4-3. Susceptibility of integrated circuits to RF tends to be more pronounced in the 20 MHz–200 MHz region. Frequencies higher than this tend to be shunted away from sensitive devices by parasitic capacitances. In general, at the IC level, the effects of RF in the region 20 MHz–200 MHz will tend to be broadband in nature, i.e., no individual frequency is more troublesome than another. However, there may be higher sensitivity to certain frequencies due to resonances on the PCB. These resonances could cause insertion gain at certain frequencies which, in turn, could cause problems for sensitive devices. By far the greatest RF signal levels are those coupled into the system via cabling. These connection points should be protected. Some techniques for protecting the system are:

1. Minimize Circuit Bandwidth
2. Isolate Sensitive Parts of the System

### Minimize Bandwidth

In this application the required analog bandwidth is only 2 kHz. This is a significant advantage when trying to reduce the effects of RF. The cable entry points can be low-pass filtered to reduce the amount of RF radiation entering the system. The shunt output is already filtered before being connected to the AD7755. This is to prevent aliasing effects that were described earlier. By choosing the correct components and adding some additional components (e.g., ferrite beads) these antialias filters can double as very effective RF filters. Figure 7 shows a somewhat idealized frequency response for the antialias filters on the analog inputs. When considering higher frequencies (e.g., > 1 MHz), the parasitic reactive elements of each lumped component must be considered. Figure 20 shows the antialias filters with the parasitic elements included. These small values of parasitic capacitance and inductance become significant at higher frequencies and therefore must be considered.

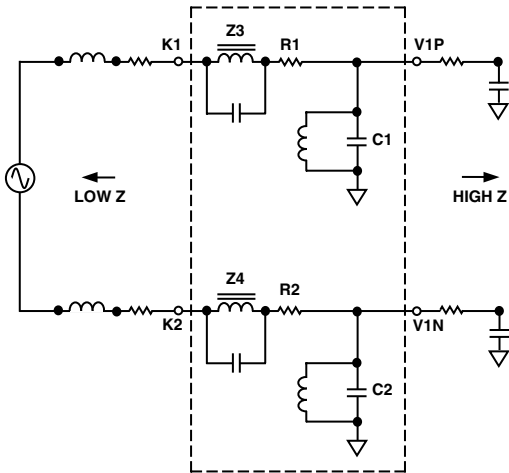


Figure 20. Antialias Filters Showing Parasitics

Parasitics can be kept at a minimum by using physically small components with short lead lengths (i.e., surface mount). Because the exact source impedance conditions are not known (this will depend on the source impedance of the electricity supply), some general precautions should be taken to minimize the effects of potential resonances. Resonances that result from the interaction of the source impedance and filter networks could cause insertion gain effects and so increase the exposure of the system to RF radiation at certain (resonant) frequencies. Lossy (i.e., having large resistive elements) components like capacitors with lossy dielectric (e.g., Type X7R) and ferrite are ideal components for reducing the “Q” of the input network. The RF radiation is dissipated as heat, rather than being reflected or diverted to another part of the system. The ferrite beads Z3 and Z4 perform very well in this respect. Figure 21 shows how the impedance of the ferrite beads varies with frequency.

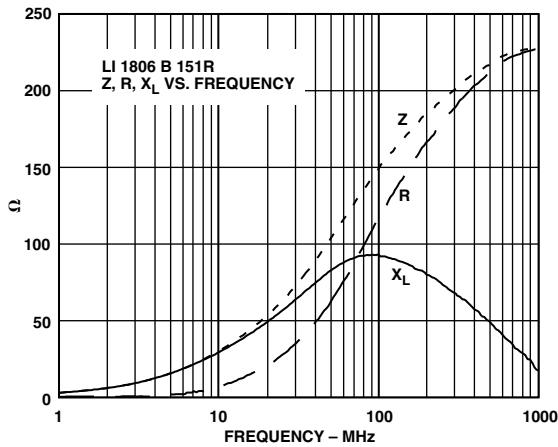


Figure 21. Frequency Response of the Ferrite Chips (Z3 and Z4) in the Antialias Filter

From Figure 21 it can be seen that the ferrite material becomes predominately resistive at high frequencies. Note also that the impedance of the ferrite material

increases with frequency, causing only high (RF) frequencies to be attenuated.

**Isolation**

The shunt connection is the only location where the AD7755 is connected directly (via antialias filters) to the “outside world.” The system is also connected to the phase and neutral lines for the purpose of generating a power supply and voltage channel signal (V2). The ferrite bead (Z1) and line filter capacitor (C16) should significantly reduce any RF radiation on the power supply.

Another possible path for RF is the signal ground for the system. A moating technique has been used to help isolate the signal ground surrounding the AD7755 from the external ground reference point (K4). Figure 22 illustrates the principle of this technique called partitioning or “moating.”

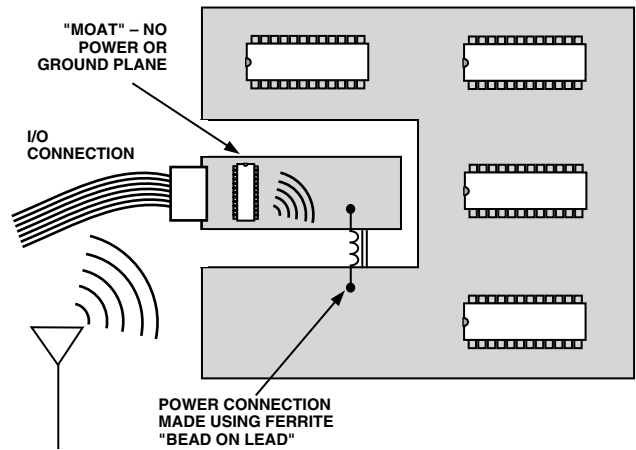


Figure 22. High-Frequency Isolation of I/O Connections Using a “Moat”

Sensitive regions of the system are protected from RF radiation entering the system at the I/O connection. An area surrounding the I/O connection does not have any ground or power planes. This limits the conduction paths for RF radiation and is called a “moat.” Obviously power, ground, and signal connections must cross this moat and Figure 22 shows how this can be safely achieved by using a ferrite bead. Remember that ferrite offers a large impedance to high frequencies (see Figure 21).

**ELECTRICAL FAST TRANSIENCE (EFT) BURST TESTING**

This testing determines the immunity of a system to conducted transients. Testing is carried out in accordance with IEC1000-4-4 under well-defined conditions. The EFT pulse can be particularly difficult to guard against because the disturbance is conducted into the system via external connections, e.g., power lines. Figure 23 shows the physical properties of the EFT pulse used in IEC1000-4-4. Perhaps the most debilitating attribute of the pulse is not its amplitude (which can be as high as 4 kV), but

the high-frequency content due to the fast rise times involved. Fast rise times mean high-frequency content which allows the pulse to couple to other parts of the system through stray capacitance, etc. Large differential signals can be generated by the inductance of PCB traces and signal ground. These large differential signals could interrupt the operation of sensitive electronic components. Digital systems are generally most at risk because of data corruption. Analog electronic systems tend only to be affected for the duration of the disturbance.

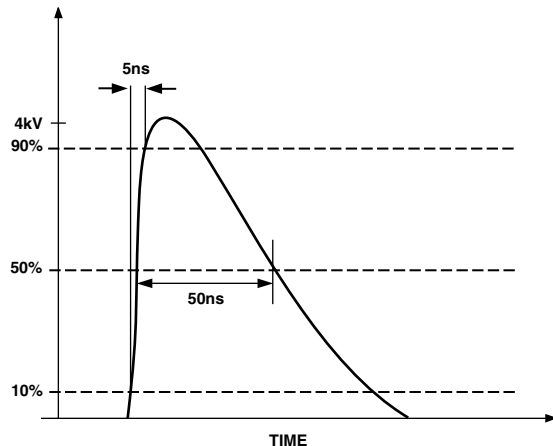


Figure 23. Single EFT Pulse Characteristics

Another possible issue with conducted EFT is that the effects of the radiation will, like ESD, generally be cumulative for electronic components. The energy in an EFT pulse can be as high as 4 mJ and deliver 40 A into a 50  $\Omega$  load (see Figure 26). Therefore continued exposure to EFT due to inductive load switching etc., may have implications for the long-term reliability of components. The best approach is to protect those parts of the system that could be sensitive to EFT.

The protection techniques described in the last section (Electromagnetic HF Fields) also apply equally well in the case of EFT. The electronics should be isolated as much as possible from the source of the disturbance through PCB layout (i.e., moating) and filtering signal and power connections. In addition, a 10 nF capacitor (C16) placed across the mains provides a low impedance shunt for differential EFT pulses. Stray inductance due to leads and PCB traces will mean that the MOV will not be very effective in attenuating the differential EFT pulse. The MOV is very effective in attenuating high energy, relatively long duration disturbances, e.g., due to lighting strikes, etc. The MOV is discussed in the next section.

#### MOV Type S20K275

The MOV used in this design was of type S20K275 from Siemens. An MOV is basically a voltage-dependant resistor whose resistance decreases with increasing voltage. They are typically connected in parallel with the

device or circuit being protected. During an overvoltage event they form a low-resistance shunt and thus prevent any further rise in the voltage across the circuit being protected. The overvoltage is essentially dropped across the source impedance of the overvoltage source, e.g., the mains network source impedance. Figure 24 illustrates the principle of operation.

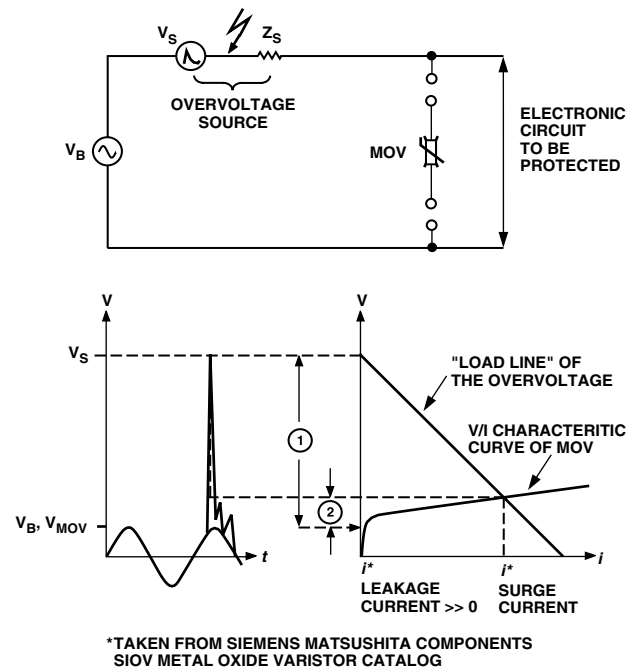


Figure 24. Principle of MOV Overvoltage Protection

The plot in Figure 24 shows how the MOV voltage and current can be estimated for a given overvoltage and source impedance. A load line (open-circuit voltage, short-circuit current) is plotted on the same graph as the MOV characteristic curve. Where the curves intersect, the MOV clamping voltage and current can be read. Note that care must be taken when determining the short-circuit current. The frequency content of the overvoltage must be taken into account as the source impedance (e.g., mains) may vary considerably with frequency. A typical impedance of 50  $\Omega$  is used for mains source impedance during fast transience (high-frequency) pulse testing. The next section discusses IEC1000-4-4 and IEC1000-4-5, which are transience and overvoltage EMC compliance tests.

#### IEC1000-4-4 and the S20K275

While the graphical technique just described is useful, an even better approach is to use simulation to obtain a better understanding of MOV operation. EPCOS Components provides SPICE models for all their MOVs and these are very useful in determining device operation under the various IEC EMC compliance tests. For more information on EPCOS SPICE models and their applications see:

<http://www.epcos.de/inf/70/e0000000.htm>

The purpose of IEC1000-4-4 is to determine the effect of repetitive, low energy, high-voltage, fast rise time pulses on an electronic system. This test is intended to simulate transient disturbances such as those originating from switching transience (e.g., interruption of inductive loads, relay contact bounce, etc.).

Figure 25 shows an equivalent circuit intended to replicate the EFT test pulse as specified in IEC1000-4-4. The generator circuit is based on Figure 1 IEC1000-4-4 (1995-01). The characteristics of operation are:

- Maximum energy of 4 mJ/pulse at 2 kV into 50 Ω
- Source impedance of 50 Ω ± 20%
- DC blocking capacitor of 10 nF
- Pulse rise time of 5 ns ± 30%
- Pulse duration (50% value) of 50 ns ± 30%
- Pulse shape as shown in Figure 23.

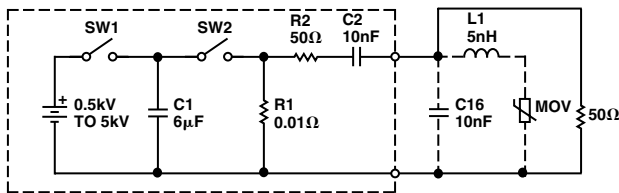


Figure 25. EFT Generator

The simulated output of this generator delivered to a purely resistive 50 Ω load is shown in Figure 26. The open-circuit output pulse amplitude from the generator is 4 kV. Therefore, the source impedance of the generator is 50 Ω as specified by the IEC1000-4-4, i.e., ratio of peak pulse output unloaded and loaded (50 Ω) is 2:1.

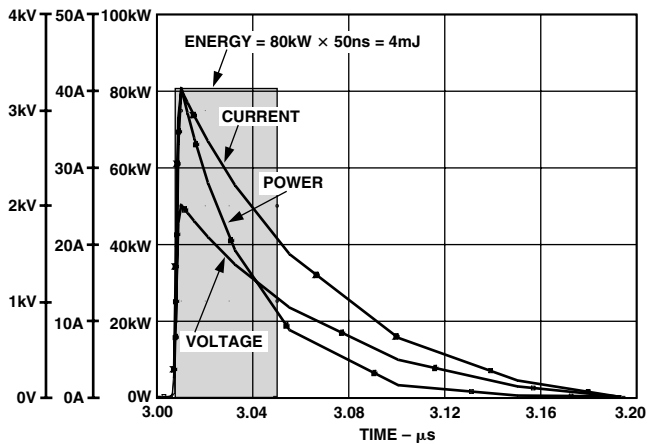


Figure 26. EFT Generator Output into 50 Ω (No Protection)

The plot in Figure 26 also shows the current and instantaneous power ( $V \times I$ ) delivered to the load. The total energy is the integral of the power and can be approximated by the rectangle method as shown. It is approximately 4 mJ at 2 kV as per specification.

Figure 27 shows the generator output into 50 Ω load with the MOV and some inductance (5 nH). This is included to take into account stray inductance due to PCB traces and leads. Although the simulation result shows that the EFT pulse has been attenuated (600 V) and most of the energy being absorbed by the MOV (only 0.8 mJ is delivered to the 50 Ω load) it should be noted that stray inductance and capacitance could render the MOV useless. For example Figure 28 shows the same simulation with the stay inductance increased to 1 µH, which could easily happen if proper care is not taken with the layout. The pulse amplitude reaches 2 kV once again.

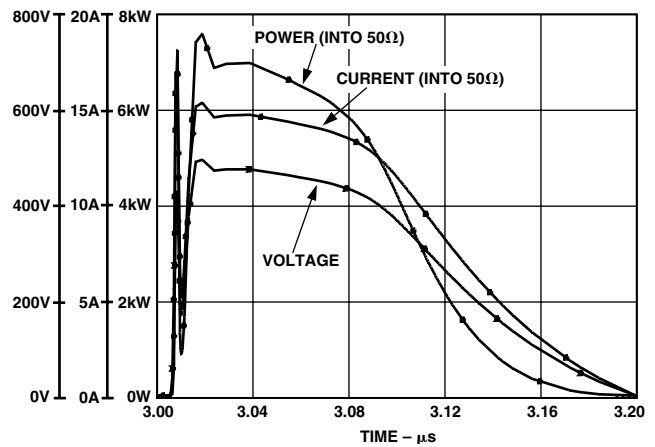


Figure 27. EFT Generator Output into 50 Ω with MOV in Place

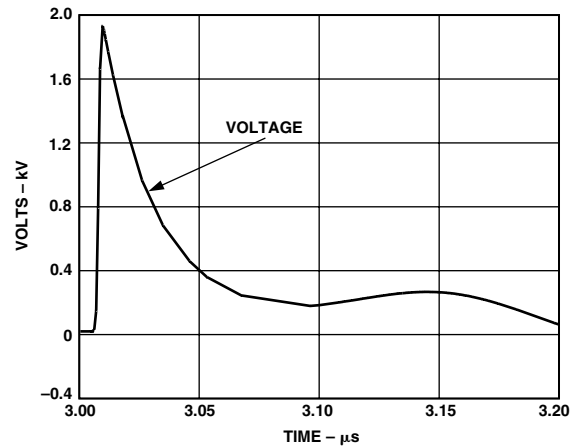


Figure 28. EFT Generator Output into 50 Ω with MOV in Place and Stray Inductance of 1 µH

When the 10 nF Capacitor (C16) is connected, a low impedance path is provided for differential EFT pulses. Figure 29 shows the effect of connecting C16. Here the stray inductance (L1) is left at 1 µH and the MOV is in place. The plot shows the current through C16 and the voltage across the 50 Ω load. The capacitor C16 provides a low impedance path for the EFT pulse. Note the peak current through C16 of 80 A. The result is that the amplitude of the EFT pulse is greatly attenuated.

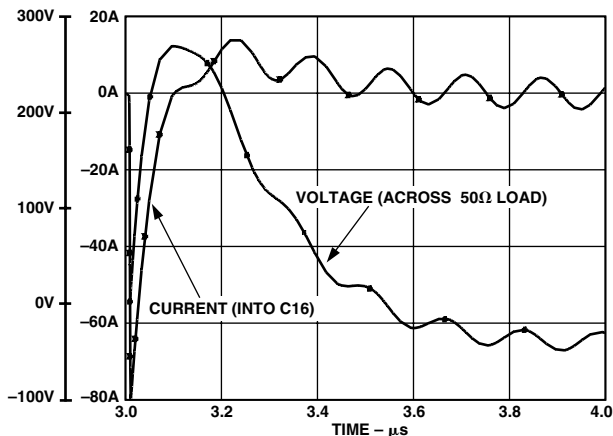


Figure 29. EFT Generator Output into 50 Ω with MOV in Place, Stray Inductance of 1 μH and C16 (10 nF) in Place

**IEC1000-4-5**

The purpose of IEC1000-4-5 is to establish a common reference for evaluating the performance of equipment when subjected to high-energy disturbances on the power and interconnect lines. Figure 30 shows a circuit that was used to generate the combinational wave (hybrid) pulse described in IEC1000-4-5. It is based on the circuit shown in Figure 1 of IEC1000-4-5 (1995-02). Such a generator produces a 1.2 μs/50 μs open-circuit voltage waveform and an 8 μs/20 μs short circuit current waveform, which is why it is referred to as a hybrid generator. The surge generator has an effective output impedance of 2 Ω. This is defined as the ratio of peak open-circuit voltage to peak short-circuit current.

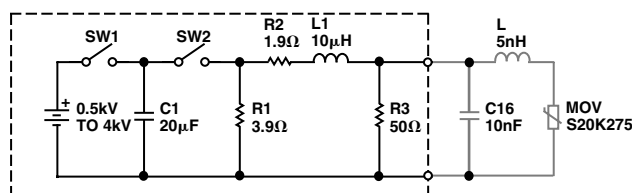


Figure 30. Surge Generator (IEC1000-4-5)

Figure 31 shows the generator voltage and current output waveforms. The characteristics of the combination wave generator are:

**Open Circuit Voltage:**

- 0.5 kV to at least 4.0 kV
- Waveform as shown in Figure 31
- Tolerance on open-circuit voltage is ±10%.

**Short-Circuit Current:**

- 0.25 kA to 2.0 kA
- Waveform as shown in Figure 31
- Tolerance on short-circuit current is ±10%.

Repetition rate of a least 60 seconds.

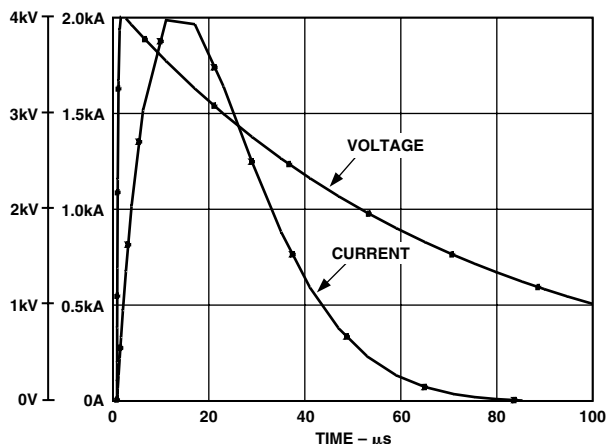


Figure 31. Open-Circuit Voltage/Short-Circuit Current

The MOV is very effective in suppressing these kinds of high energy/long duration surges. Figure 32 shows the voltage across the MOV when it is connected to the generator as shown in Figure 30. Also shown are the current and instantaneous power waveform. The energy absorbed by the MOV is readily estimated using the rectangle method as shown.

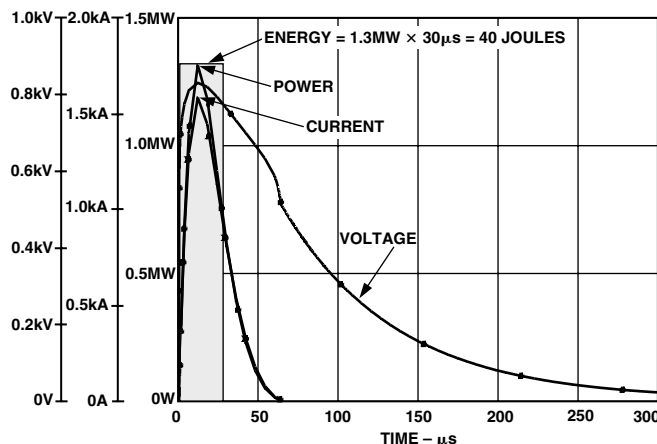


Figure 32. Energy Absorbed by MOV During 4 kV Surge

**Derating the MOV Surge Current**

The maximum surge current (and, therefore, energy absorbed) that an MOV can handle is dependant on the number of times the MOV will be exposed to surges over its lifetime. The life of an MOV is shortened every time it is exposed to a surge event. The data sheet for an MOV device will list the maximum nonrepetitive surge current for an 8 μs/20 μs current pulse. If the current pulse is of longer duration, and if it occurs more than once during the life of the device, this maximum current must be derated. Figure 33 shows the derating curve for the S20K275. Assuming exposures of 30 μs duration, and a peak current as shown in Figure 32, the maximum number of surges the MOV can handle before it goes out of specification is about 10. After repeated loading (10 times in the case just described) the MOV voltage will change. After initially increasing, it will rapidly decay.

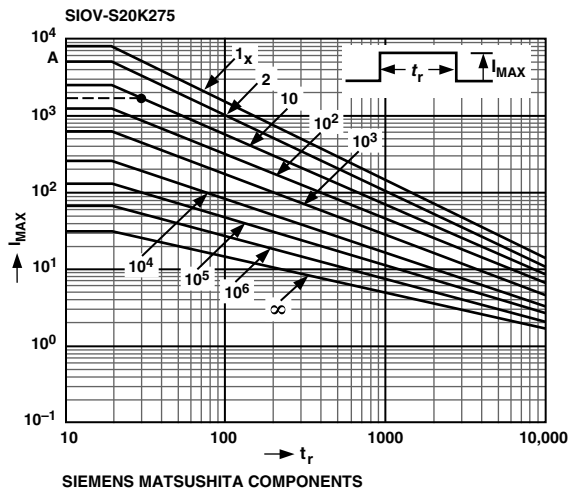


Figure 33. Derating Curve for S20K275

### EMC Test Results

The reference design has been fully tested for EMC at an independent test house. Testing was carried out by Integrity Design & Test Services Inc., Littleton, MA 01460, USA. The reference design was also evaluated for Emissions (EN 55022 Class B) pursuant to IEC 1036:1996 requirements. A copy of the test report can be obtained from the Analog Devices website at:

[http://www.analog.com/techsupt/application\\_notes/ad7755/64567\\_e1.pdf](http://www.analog.com/techsupt/application_notes/ad7755/64567_e1.pdf)

The design was also evaluated for susceptibility to electrostatic discharge (ESD), radio frequency interference (RFI), keyed radio frequency interference, and electrical fast transients (EFT), pursuant to IEC 1036:1996 requirements. The test report is available at:

[http://www.analog.com/techsupt/application\\_notes/ad7755/64567\\_c1.pdf](http://www.analog.com/techsupt/application_notes/ad7755/64567_c1.pdf)

A copy of the certification issued for the design is shown in the test results section of this application note.

### PCB DESIGN

Both susceptibility to conducted or radiated electromagnetic disturbances and analog performance were considered at the PCB design stage. Fortunately, many of the design techniques used to enhance analog and mixed-signal performance also lend themselves well to improving the EMI robustness of the design. The key idea is to isolate that part of the circuit that is sensitive to noise and electromagnetic disturbances. Since the AD7755 carries out all the data conversion and signal processing, the robustness of the meter will be determined to a large extent by how protected the AD7755 is.

In order to ensure accuracy over a wide dynamic range, the data acquisition portion of the PCB should be kept as quiet as possible, i.e., minimal electrical noise. Noise

will cause inaccuracies in the analog-to-digital conversion process that takes place in the AD7755. One common source of noise in any mixed-signal system is the ground return for the power supply. Here high-frequency noise (from fast edge rise times) can be coupled into the analog portion of the PCB by the common impedance of the ground return path. Figure 34 illustrates the mechanism.

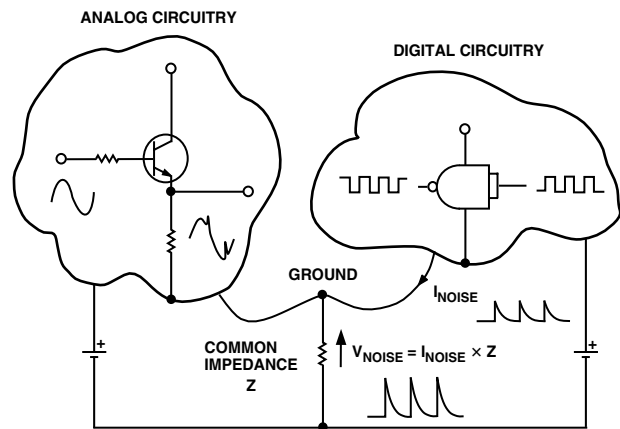


Figure 34. Noise Coupling via Ground Return Impedance

One common technique to overcome these kinds of problems is to use separate analog and digital return paths for the supply. Also, every effort should be made to keep the impedance of these return paths as low as possible. In the PCB design for the AD7755, separate ground planes were used to isolate the noisy ground returns. The use of ground plane also ensures the impedance of the ground return path is kept as very low.

The AD7755 and sensitive signal paths are located in a “quiet” part of the board that is isolated from the noisy elements of the design like the power supply, flashing LED, etc. Since the PSU is capacitor-based, a substantial current (approximately 32 mA at 220 V) will flow in the ground return back to the phase wire (system ground). This is shown in Figure 35. By locating the PSU in the digital portion of the PCB, this return current is kept away from the AD7755 and analog input signals. This current is at the same frequency as the signals being measured and could cause accuracy issues (e.g., crosstalk between the PSU as analog inputs) if care is not taken with the routing of the return current. Also, part of the attenuation network for the Channel 2 (voltage channel) is in the digital portion of the PCB. This helps to eliminate possible crosstalk to Channel 1 by ensuring analog signal amplitudes are kept as low as possible in the analog (“quiet”) portion of the PCB. Remember that with a shunt size of 350  $\mu\Omega$ , the voltage signal range on Channel 1 is 35  $\mu\text{V}$  to 14 mV (2% Ib to 800% Ib). Figure 35 shows the PCB floor plan which was eventually adopted for the watt-hour meter.

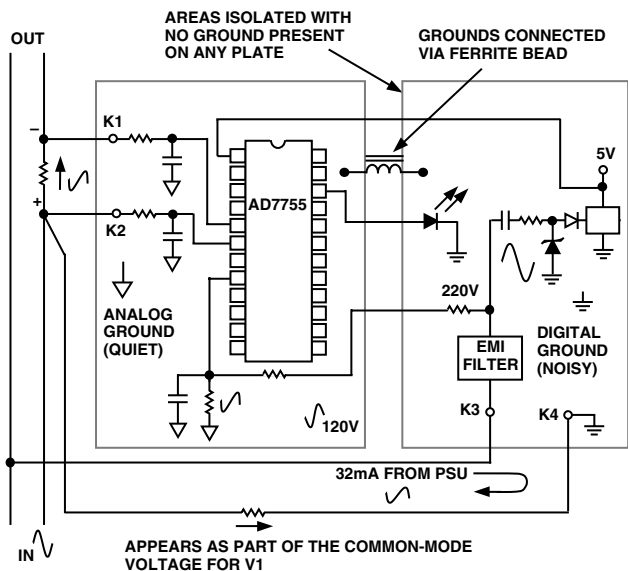


Figure 35. AD7755 Watt-Hour Meter PCB Design

The partitioning of the power planes in the PCB design as shown in Figure 35 also allows us to implement the idea of a “moat” for the purposes of immunity to electromagnetic disturbances. The digital portion of the PCB is the only place where both phase and neutral wires are connected. This portion of the PCB contains the transience suppression circuitry (MOV, ferrite, etc.) and power supply circuitry. The ground planes are connected via a ferrite bead that helps to isolate the analog ground from high-frequency disturbances (see Design For Immunity to Electromagnetic Disturbances section).

**METER ACCURACY/TEST RESULTS**

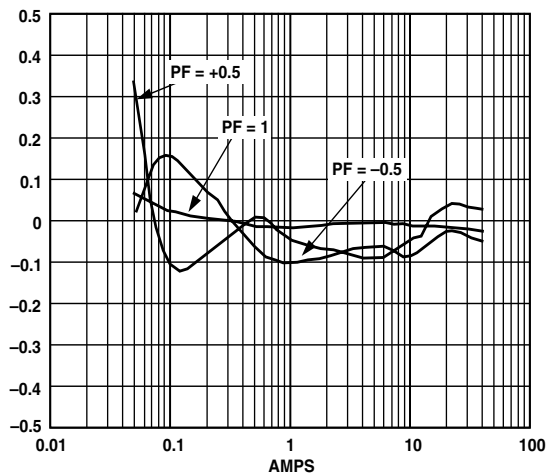


Figure 36. Measurement Error (% Reading) @ 25°C, 220 V, PF = +0.5/-0.5, Frequency = 50 Hz

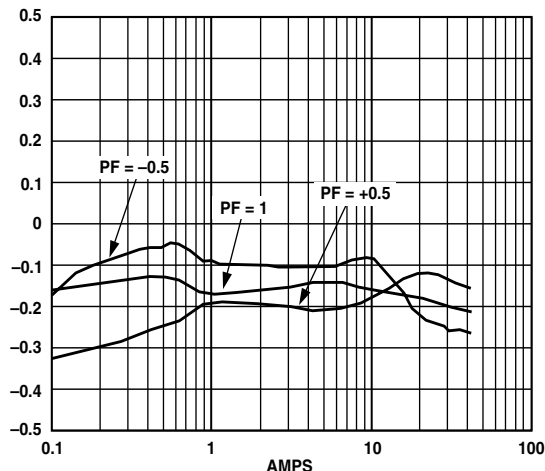


Figure 37. Measurement Error (% Reading) @ 70°C, 220 V, PF = +0.5/-0.5, Frequency = 50 Hz

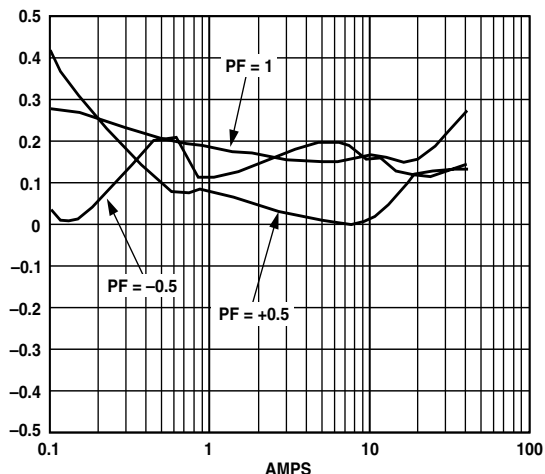


Figure 38. Measurement Error (% Reading) @ -25°C, 220 V, PF = +0.5/-0.5, Frequency = 50 Hz

**EMISSIONS TESTING (EMC) N55022:1994**

At end of data sheet.

**SUSCEPTIBILITY TESTING (EMC) EN 61000-4-2, EN 61000-4-3, EN 61000-4-4, ENV 50204**

At end of data sheet.

**ANSI C12.16 AND IEC1039**

The ANSI standard governing Solid-State Electricity Meters is ANSI C12.16-1991. Since this application note refers to the IEC 1036 specifications when explaining the design, this section will explain some of those key IEC1036 specifications in terms of their ANSI equivalents. This should help eliminate any confusion caused by the different application of some terminology contained in both standards.

## **Class—IEC1036**

The class designation of an electricity meter under IEC1036 refers to its accuracy. For example a Class 1 meter will have a deviation from reference performance of no more than 1%. A Class 0.5 meter will have a maximum deviation of 0.5% and so on. Under ANSI C12.16 Class refers to the maximum current the meter can handle for rated accuracy. The given classes are: 10, 20, 100, 200 and 320. These correspond to a maximum meter current of 10 A, 20 A, 100 A, 200 A and 320 A respectively.

## **I<sub>basic</sub> (I<sub>b</sub>)—IEC1036**

The basic current (I<sub>b</sub>) is a value of current with which the operating range of the meter is defined. IEC1036 defines the accuracy class of a meter over a specific dynamic range, e.g.,  $0.05 I_b \leq I \leq I_{MAX}$ . It is also used as the test load when specifying the maximum permissible effect of influencing factors, e.g., voltage variation and frequency variation. The closest equivalent in ANSI C12.16 is the Test Current. The Test Current for each meter class (maximum current) is given below:

Class 10 : 2.5 A  
Class 20 : 2.5 A  
Class 100 : 15 A  
Class 200 : 30 A  
Class 320 : 50 A

## **I<sub>MAX</sub>—IEC1036**

I<sub>MAX</sub> is the maximum current for which the meter meets rated accuracy. This would correspond to the meter class under ANSI C12.16. For example a meter with an I<sub>MAX</sub> of 20 A under IEC 1026 would be designated Class 20 under ANSI C12.16.

## **NO LOAD THRESHOLD**

The AD7755 has on-chip anticreep functionality. The AD7755 will not produce a pulse on CF, F1, or F2 if the output frequency falls below a certain level. This feature ensures that the energy meter will not register energy when no load is connected. IEC 1036 (1996-09) section 4.6.4 specifies the start-up current as being not more than 0.4% I<sub>b</sub> at PF = 1. For this design the start current is calculated at 7.8 mA or 0.16% I<sub>b</sub>—see No Load Threshold section in the AD7755 data sheet.



## Bill of Materials

Part(s)	Details	Comments
R1, R2, R3, R4	1 k $\Omega$ , 1%, 1/8 W	SMD 1206 Resistor Surface Mount, Panasonic ERJ-8ENF1001 Digi-Key No. P 1K FCT-ND
R5	300 k $\Omega$ , 5%, 1/2 W, 200 V	SMD 2010 Resistor Surface Mount, Panasonic, ERJ-12ZY304 Digi-Key No. P 300K WCT-ND
R6	150 k $\Omega$ , 5%, 1/2 W, 200 V	SMD 1210 Resistor Surface Mount, Panasonic, ERJ-14YJ154 Digi-Key No. P 150K VCT-ND
R7	75 k $\Omega$ , 5%, 1/8 W, 200 V	SMD 1206 Resistor Surface Mount, Panasonic, ERJ-8GEYJ753 Digi-Key No. P 75K ECT-ND
R8	39 k $\Omega$ , 5%, 1/16 W, 50 V	SMD 0402 Resistor Surface Mount, Panasonic, ERJ-2GEJ393 Digi-Key No. P 39K JCT-ND
R9	18 k $\Omega$ , 5%, 1/16 W, 50 V	SMD 0402 Resistor Surface Mount, Panasonic, ERJ-2GEJ183 Digi-Key No. P 18K JCT-N
R10	9.1 k $\Omega$ , 5%, 1/16 W, 50 V	SMD 0402 Resistor Surface Mount, Panasonic, ERJ-2GEJ912 Digi-Key No. P 9.1K JCT-ND
R11	5.1 k $\Omega$ , 5%, 1/16 W, 50 V	SMD 0402 Resistor Surface Mount, Panasonic, ERJ-2GEJ512 Digi-Key No. P 5.1K JCT-ND
R12	2.2 k $\Omega$ , 5%, 1/16 W, 50 V	SMD 0402 Resistor Surface Mount, Panasonic, ERJ-2GEJ222 Digi-Key No. P 2.2K JCT-ND
R13	1.2 k $\Omega$ , 5%, 1/16 W, 50 V	SMD 0402 Resistor Surface Mount, Panasonic, ERJ-2GEJ122 Digi-Key No. P 1.2K JCT-ND
R14	560 $\Omega$ , 5%, 1/16 W, 50 V	SMD 0402 Resistor Surface Mount, Panasonic, ERJ-2GEJ561 Digi-Key No. P 560 JCT-ND
R15, R16	330 k $\Omega$ , 5%, 1/2 W, 200 V	SMD 2010 Resistor Surface Mount, Panasonic, ERJ-12ZY334 Digi-Key No. P 330K WCT-ND
R17, R23	1 k $\Omega$ , 5%, 1/8 W, 200 V	SMD 1206 Resistor Surface Mount, Panasonic, ERJ-8GEYJ102 Digi-Key No. P 1K ECT-ND
R18	820 $\Omega$ , 5%, 1/8 W, 200 V	SMD 1206 Resistor Surface Mount, Panasonic, ERJ-8GEYJ821 Digi-Key No. P 820 ECT-ND
R19, R20	20 $\Omega$ , 5%, 1/8 W, 200 V	Resistor Surface Mount, Panasonic, ERJ-8GEYJ200 Digi-Key No. P 20 ECT-ND
R21	470 $\Omega$ , 5%, 1 W	Through-hole, Panasonic, Digi-Key No. P470W-1BK-ND
R22	10 $\Omega$ , 5%, 1/8 W, 200 V	SMD 1206 Resistor Surface Mount, Panasonic, ERJ-8GEYJ100 Digi-Key No. P 10 ECT-ND
C1, C2, C3, C4	33 nF, Multilayer Ceramic, 10% 50 V, X7R	SMD 0805 Capacitor Surface Mount, Panasonic, ECJ-2VB1H333K Digi-Key No. PCC 1834 CT-ND
C5, C13	10 $\mu$ F, 6.3 V	EIA size A Capacitor Surface Chip-Cap, Panasonic, ECS-TOJY106R Digi-Key No. PCS 1106CT-ND – 3.2 mm $\times$ 1.6 mm

# AN-559

Part(s)	Details	Comments
C6, C7, C10, C12, C14, C15, C19	100 nF, Multilayer Ceramic, 10%, 16 V, X7R	SMD 0805 Capacitor Surface Mount, Panasonic, ECJ-2VB1E104K Digi-Key No. PCC 1812 CT-ND
C8, C9	22 pF, Multilayer Ceramic, 5%, 50 V, NPO	SMD 0402 Capacitor Surface Mount, Panasonic, ECU-E1H220JCQ Digi-Key No. PCC 220CQCT-ND
C11	6.3 V, 220 μF, Electrolytic	Through-hole Panasonic, ECA-OJFQ221 Digi-Key P5604 – ND D = 6.3 mm, H = 11.2 mm, Pitch = 2.5 mm, Dia. = 0.5 mm
C16	10 nF, 250 V, Class X2	Metallized Polyester Film Through-Hole Panasonic, ECQ-U2A103MN Digi-Key No. P4601-ND
C17	470 nF, 250 V AC	Metallized Polyester Film Through-Hole Panasonic, ECQ-E6474KF Digi-Key No. EF6474-NP
C18	35 V, 470 μF, Electrolytic	Through-Hole Panasonic, ECA-1VHG471 Digi-Key P5554 – ND
U1	AD7755AN	Supplied by ADI – 24 Pin DIP, Use Pin Receptacles (P1–P24)
U2	LM78L05	National Semiconductor, LM78L05ACM, S0-8 Digi-Key LM78L05ACM-ND
U3	PS2501-1	Opto, NEC, Digi-key No PS2501-1NEC-ND
U4	AD780BRS	Supplied by ADI – 8 Pin SOIC
D1	Low Current LED	HP HLMP-D150
D2	Rectifying Diode	Newark 06F6429 (Farnell 323-123) 1 W, 400 V, DO-41, 1N4004, Digi-Key 1N4004DICT-ND
D3	Zener Diode	15 V, 1 W, DO-41, 1N4744A Digi-Key 1N4744ADICT-ND
Z1, Z2	Ferrite Bead Cores	Axial-Leaded (15 mm × 3.8 mm ) 0.6 mm Lead Diameter Panasonic, EXCELSA391, Digi-Key P9818BK-ND
Z3, Z4	Ferrite SMD Bead	SMD 1806 Steward, LI 1806 E 151 R Digi-Key 240-1030-1-ND
Y1	3.579545 MHz XTAL	Quartz Crystal, HC-49(US), ECS No. ECS-35-17-4 Digi-Key No. X079-ND
MOV1	Metal Oxide Varistors	AC 275 V, 140 Joules FARNELL No. 580-284, Siemens, S20K275
J1–J10	0.1 Ω, 5%, 1/4 W, 200 V	SMD 1210 Resistor Surface Mount, Panasonic ERJ-14RSJ0R1, Digi-Key No. P0.1SCT-ND
J11–J15	0 Ω, 5%, 1/8 W, 200 V	SMD 1206 Resistor Surface Mount, Panasonic, ERJ-8GEYJ000 Digi-Key No. P0.0ECT-ND
P1–P24	Single Low Profile	Sockets for U1 0.022" to 0.025" Pin Diameter ADI Stock 12-18-33. ADVANCE KSS100-85TG
K1–K8	Pin Receptacles	0.037" to 0.043" Pin Diameter, Hex Press Fit Mil-Max no. 0328-0-15-XX-34-XX-10-0 Digi-Key ED5017-ND
Counter	2 Phase Stepper, 100 imp	China National Electronics Import & Export Shaanxi Co. No.11 A, Jinhua northern Road, Xi'an China. Email: chenyf@public.xa.sn.cn Tel: 86-29 3218247,3221399 Fax: 86-29 3217977, 3215870

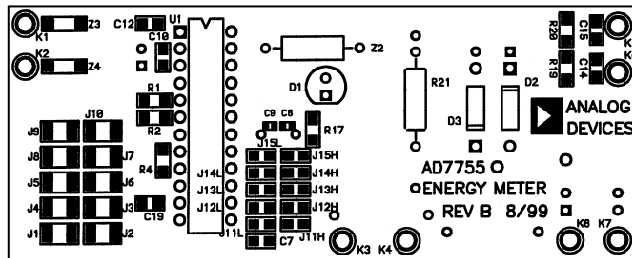


Figure 39. PCB Assembly (Top Layer)

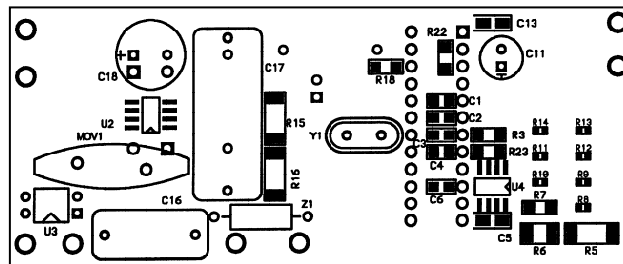


Figure 40. PCB Assembly (Bottom Layer)

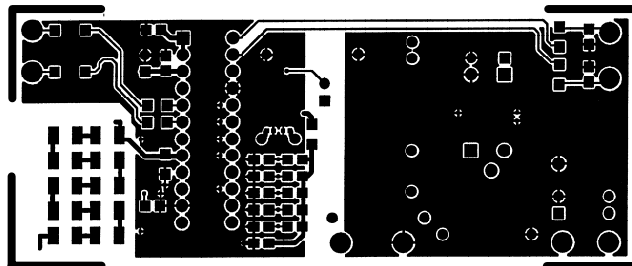


Figure 41. PCB (Top Layer)

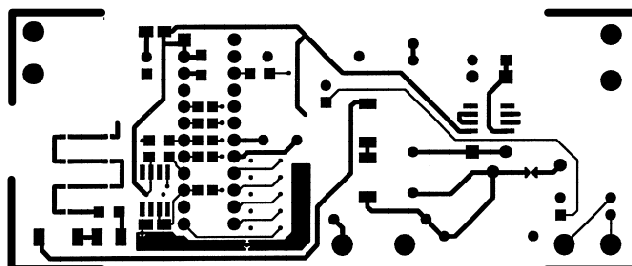


Figure 42. PCB (Bottom Layer)

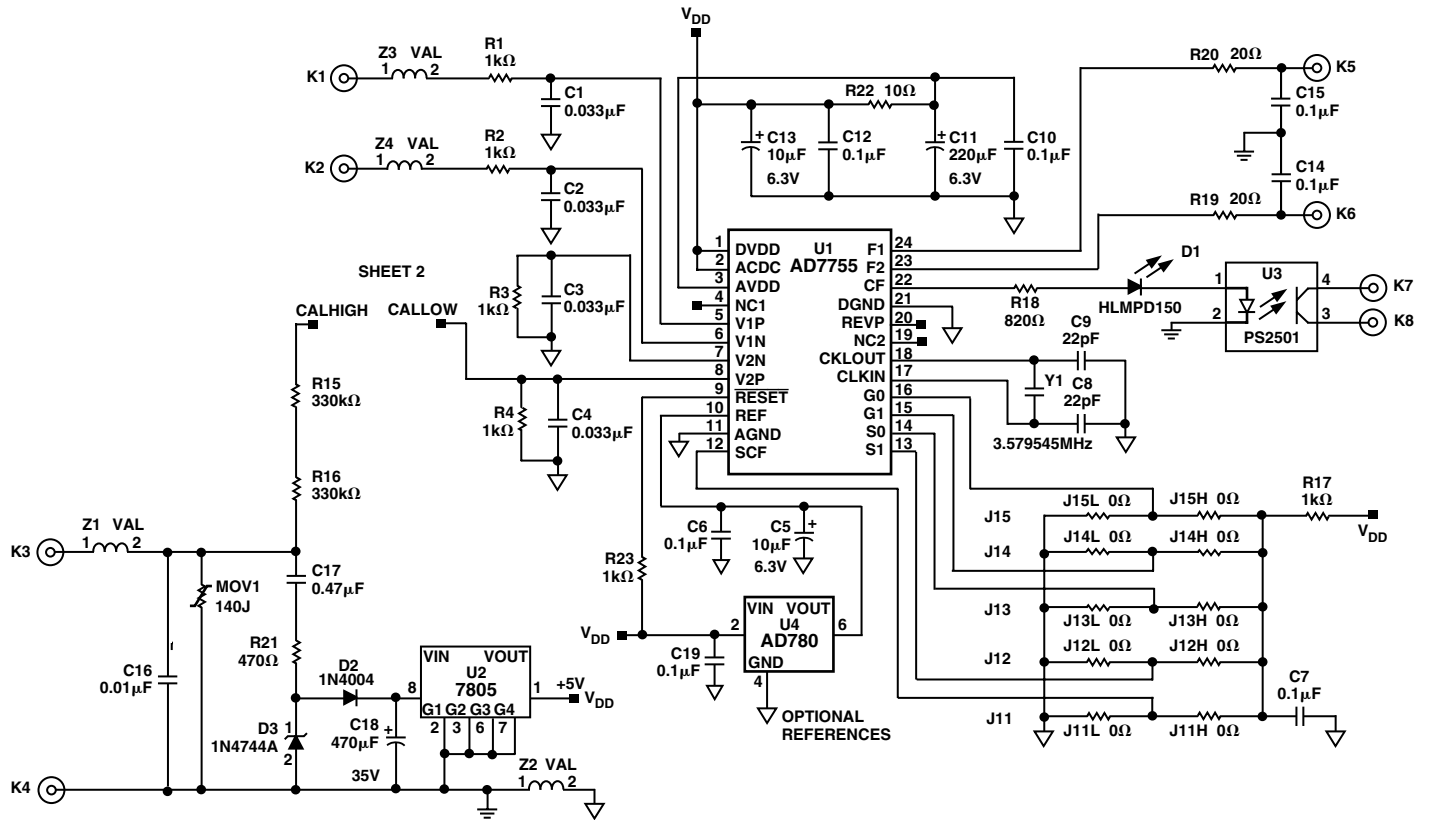


Figure 43. Schematic 1

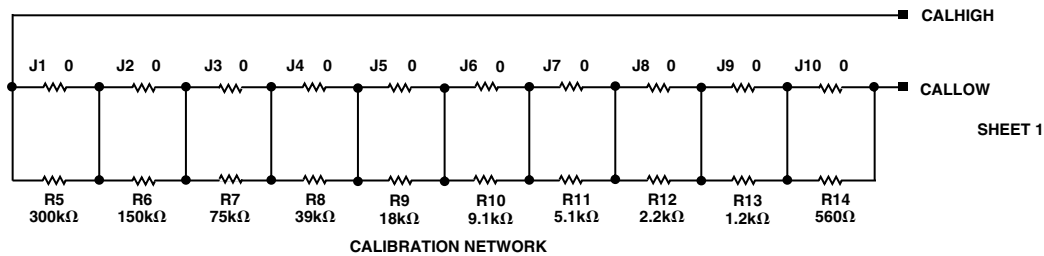


Figure 44. Schematic 2

					
<h2 style="margin: 0;">Certificate of Compliance</h2>					
<p>The following product was found to comply with the requirement stated below when tested in accordance with the test procedures described in the accompanying test/measurement report. Reference report number 64567.e1</p>					
Manufacturer:	Analog Devices, Inc. 804 Woburn Street Wilmington, MA 01887				
Model:	Energy Meter (AD7755)				
Requirement:	EN55022:1994 + A1:1995 + A2:1997, Class B				
Applicable Directive:	89/336/EEC				
Approved By:					
<table border="1" style="width: 100%;"> <tr> <td style="padding: 5px;">Robert D. Goyette NVLAP Signatory</td> <td style="text-align: center; vertical-align: middle;">  </td> </tr> <tr> <td style="text-align: center; padding: 5px;">Date</td> <td style="text-align: center; vertical-align: middle;">           9/13/99         </td> </tr> </table>	Robert D. Goyette NVLAP Signatory		Date	9/13/99	
Robert D. Goyette NVLAP Signatory					
Date	9/13/99				
Remarks:	<p><i>Testing is performed using calibrated equipment traceable to the National Institute of Standards and Technology (NIST).</i></p> <p><i>This certificate is valid for products tested as described in the accompanying test report. Specific modifications necessary to meet the above requirement, recommended by Integrity Design &amp; Test Services, Inc. are described therein.</i></p> <p style="text-align: center;"><i>Integrity Design &amp; Test Services, Inc. is accredited by the National Voluntary Laboratory Accreditation Program (NVLAP) for Electromagnetic Emissions Testing</i></p>				

Figure 45. Certificate 1, Emissions Testing





E3742-2.5-6/00 (rev. A) 01017

PRINTED IN U.S.A.

Figure 46. Certificate 2, Susceptibility